Intrinsic and hysteresis properties of FePt nanoparticles

J. A. Christodoulides, M. J. Bonder, Y. Huang, Y. Zhang, S. Stoyanov, and G. C. Hadjipanayis
Department of Physics and Astronomy, University of Delaware, Newark, Delaware 19716, USA

A. Simopoulos
Institute of Material Science, National Center for Scientific Research Demokritos, Ag. Paraskevi Attiki, 159 10 Greece

D. Weller
Seagate Technology, Pittsburgh, Pennsylvania 15203, USA

(Received 30 May 2002; revised manuscript received 1 May 2003; published 27 August 2003)

This comprehensive study examines the effect of particle size and atomic ordering on the intrinsic and hysteresis properties of FePt nanoparticles embedded in a carbon matrix formed by annealing sputtered FePt/C multilayer precursors. Structural studies show a transformation from the magnetically soft to the tetragonal FePt phase dependent on the annealing conditions. The magnetic properties scale as a function of particle size. The coercivity depends, in part, on the vol % of carbon and develops with annealing as a result of increased atomic ordering. Under the right conditions a high coercivity of 34 kOe has been achieved. Remanence curves show a variation of interparticles interactions from exchange to magnetostatic with increasing vol % carbon. Time dependent measurements indicate a decrease of the activation volume converging to the actual particle size (determined by TEM) as the carbon content is increased. The potential for future magnetic recording media is discussed.

DOI: 10.1103/PhysRevB.68.054428 PACS number(s): 75.75.+a

I. INTRODUCTION

The recent explosion of work in nanoparticle systems is due to both the physics of the enhanced properties as a material is reduced in size and to the technological possibilities associated with the improved properties. These include increased coercivity and enhanced magnetization to superparamagnetism for magnetic nanoparticles.[1–4] The prime technological example is magnetic recording media. The magnetic recording industry has enjoyed a doubling of areal densities every 12–18 months for the last decade. Such growth has been facilitated by advances in the understanding of these materials as they approach the nanoscale size regime. In order to maintain this phenomenal pace of growth in information storage density there is a fundamental barrier to further reducing the size of written bits. This is due to the superparamagnetic limit. As a magnetic material is reduced in dimension the influence of thermal energy begins to dominate.[3] The thermal stability is reduced and the spins within the particle randomize in the absence of a field and hence the data is no longer stored. Superparamagnetism is predicated on the height KV of the energy barrier associated with the reversal of magnetization where K is the anisotropy energy density of the material in question and V is the effective volume being reversed. In order to maintain a written bit for an acceptable length of time, the relation $KV \geqslant 50-70\,\mathrm{kT}$ must be satisfied.[3] Thus the crux of the problem lies in the fact that we must simultaneously reduce the bit size and increase the anisotropy to increase the areal density. The magnetic recording industry has responded with a number of possible solutions. These include perpendicular recording,[5] patterned media,[6] antiferromagnetically coupled media,[7,8] and the use of materials with higher anisotropy.[3]

The focus of this paper is on the high anisotropy FePt $L1_0$ nanomaterial. The FePt system is well established as having exceptional properties in the bulk,[9] and has been extensively studied in thin film form.[10–27] The system has been studied as single layers[20–22] and multilayers with bilayers constituents of Ag,[11,12,19,23,25] C,[10,11,15,24] BN,[10] SiO_2,[13] and Al_2O_3.[19] These properties coupled with the fact that the alloys are highly oxidation resistant make them ideal candidates for future magnetic recording media. Along with the technological prospects there are intrinsic properties affected by the reduction of particle size such as the anisotropy, the saturation magnetization and Curie temperature.[26] In Sec. II we discuss the experimental procedures including the formation of the nanoparticles being studied, the sample characterization techniques and the sample deposition parameters. In Sec. III the results will be discussed. Finally, in Sec. IV a summary is given that discusses the fundamental and technological implications of the work presented.

II. EXPERIMENT

Fabrication of nanoparticles in a carbon matrix was accomplished by utilizing multilayer precursors consisting of stacks of FePt/C bilayers, followed by a heat treatment that breaks the layers and leads to the formation of the nanoparticles. Samples were deposited by varying the thickness of the constituent layers of FePt between 3 and 10 Å and the Carbon layer thickness between 3 and 40 Å. An ultrahigh vacuum compatible sputter deposition chamber with a base pressure of 2×10^{-7} Torr was used to deposit samples in an Ar pressure of 5 mTorr. Annealing of the multilayers was carried out under vacuum using temperatures in the range of 600–800 °C for times between 2 min and 3 h.

Magnetic data was acquired using a superconducting quantum interference device (SQUID) magnetometer and an

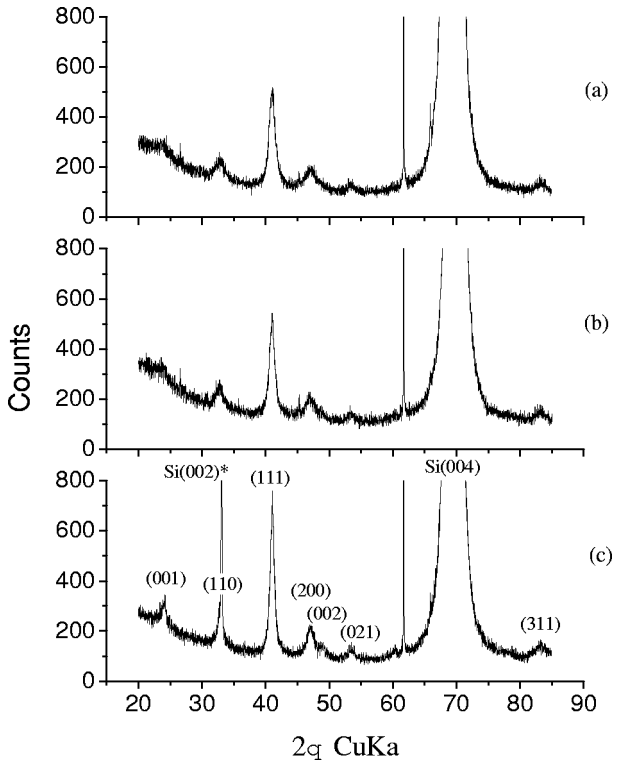

FIG. 1. X-ray pattern of FePt/C with 58.3-vol % C, annealed at 600 °C for (a) 30, (b) 60, and (c) 120 min.

Oxford vibrating sample magnetometer (VSM). X-Ray Diffraction (XRD) patterns were taken with a Philips CM20 diffractometer using Cu $K\alpha$ radiation. Electron microscopy micrographs were produced using a Jeol JEM-2000FX TEM while high-resolution microscopy was carried out on a Phillips 20CM Field Emission Gun (FEG) electron microscope equipped with energy dispersive x-ray spectroscopy for elemental analysis. Moessbauer spectra were taken at room temperature (RT) and liquid nitrogen (LN) temperatures. The overall multilayer thickness was regulated to amount to a FePt thickness of 1500 Å for all samples studied. Stacks of four films with dimensions 1×1 cm^2 were used as absorbers. Spectra with an absorption of $\sim0.5\%$ were achieved in this way. Isomer shift values are given with respect to Fe metal at RT. The Fe target was enriched by $\sim20\%$ Fe^{57} in order to improve the signal to noise ratio.

III. RESULTS AND DISCUSSION

Structural measurements

The XRD spectra of all as-deposited FePt films clearly show a disordered amorphous-like fcc structure with a lattice constant of $a=3.81$ Å. Annealing at different temperatures and aging times transformed the as deposited material into the desired ordered face centered tetragonal phase (fct). The onset of ordering was observed when the samples were annealed at 600 °C. This was evident in the x-ray patterns with the appearance of the superlattice reflections (001) and (110) at 2θ angles of about 24° and 33°, respectively. Figure 1 shows the XRD patterns of FePt/C with 58.3 vol % of C annealed at 600 °C at three different annealing times. As the annealing time increases, the intensity of the superlattice peaks concurrently increases indicating the increase in the degree of ordering in the samples. There is also narrowing of the XRD peaks, indicative of grain growth. Further confirmation of chemical ordering can be seen as a result of the splitting of the (200) and (311) lines to give the (002) and (113) lines, respectively.

TABLE I. Parameters used to estimate the degree of order, S_0 for FePt.

Peak	LP	M_{Fe}	f_{Fe}	I_{Fe}	M_{Pt}	f_{Pt}	I_{Pt}
(001)	2.26	0.005	21.01	3.4	0.005	64.43	8.0
(002)	0.94	0.019	16.93	3.3	0.018	55.12	7.0
(003)	0.54	0.043	12.86	3.3	0.041	45.81	7.0

The disordered fcc to ordered fct transformation involves a decrease in dimensions along the c axis and an increase along a and b axes, leading to tetragonality with the aspect ratio $c/a<1$. The degree of atomic ordering, S_0, can be determined directly by comparing the diffracted x-ray integrated intensities of the fundamental and superstructure reflections consistent with the formalism given by Warren[28] using the parameters in Table I.

The phase transformation to the high anisotropy fct structure is critical for the development of the magnetic properties of interest from both the magnetic recording standpoint as well as the study of the intrinsic size effects. The linear dependence of S_0 versus the inverse grain size, as shown in Fig. 2, clearly shows the size effect on the chemical ordering. The larger grains have a higher degree of chemical ordering. In this sense one can argue that in the early aging stages each individual grain consists of regions of both the ordered and disordered structure. As its size increases, the ordered fraction of the grain increases at the expense of the disordered ones. These results are consistent with Mossbauer measurements presented in this section.

Microstructural measurements

All the samples start out as multilayers with a distinct periodicity that is destroyed after annealing. Figure 3 shows

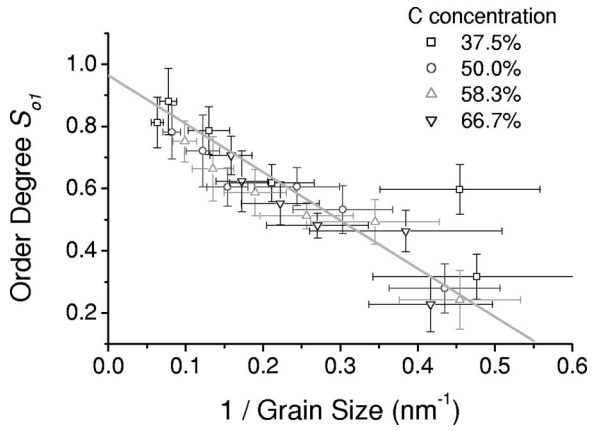

FIG. 2. Degree of atomic ordering as a function of 1/grain size for FePt/C samples with different C content.

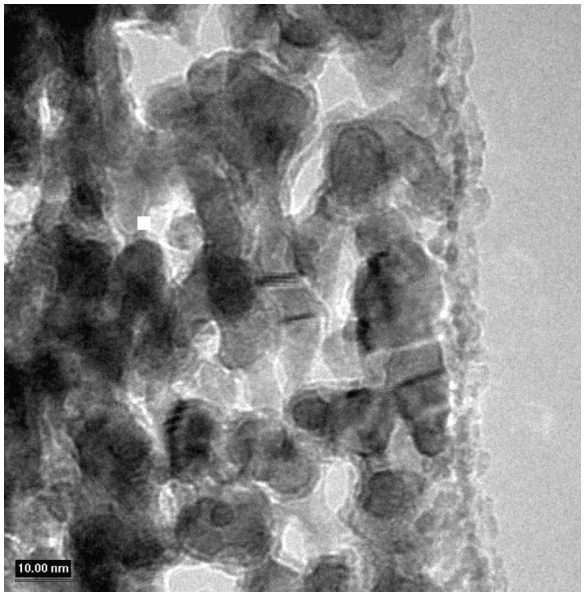

FIG. 3. High resolution TEM bright field image of a FePt/C multilayer annealed at 700 °C for 10 min.

a cross sectional high resolution TEM image of a FePtPt(12 Å)/C(12 Å) multilayer annealed at 700 °C for 10 min. The micrograph shows no evidence of a multilayer structure even after only 10 min of annealing. The particles are almost spherical in shape with an average particle size of about 10 nm. In addition, the particles have grown across the layers, as the as-deposited layers were only 12 Å thick. Bright field TEM images of planar samples show increased particle size as as seen in Figs. 4(a)–4(d) for a sample with 58.3-vol % C

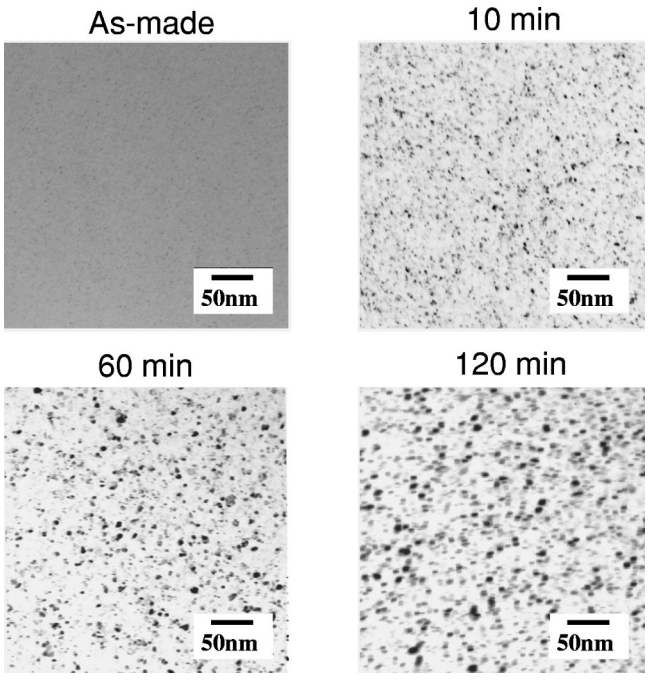

FIG. 4. TEM bright field images for a FePt/C sample with 58.3-vol % C annealed at 600 °C for (a) as made, (b) 10, (c) 60, and (d) 120 min.

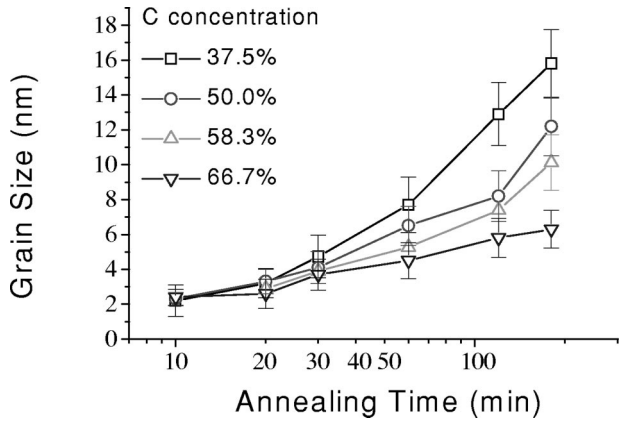

FIG. 5. Variation of grain size with annealing time for the vol % C listed.

annealed at 600 °C for increasing lengths of time. The data show that not only does the particle size become larger with prolonged annealing time (progressing from a fine grained microstructure to a particulate system with 10-nm particles), but the spacing of the particles becomes larger. The role of carbon with respect to the structure is two-fold. It inhibits particle growth as well as separates the particles from one another. This increase in the interparticle distances has an effect on the magnetic interaction between particles as will be shown in the next section. The effect of particle growth inhibitor is best seen in a plot of the grain size vs annealing time for several different values of C vol %, as shown in Fig. 5. As can be seen in the figure the grain sizes are reduced with increasing carbon content. Thus the amount of carbon was varied in an effort to keep the particle size within the range required for magnetic recording media and to increase the percentage of fct in the material. This, as will be shown in the next section, has advantageous effects on the coercivity.

Magnetic properties

This section looks at some of the magnetic properties of interest such as the magnetization, magneto-crystalline anisotropy, coercivity and viscosity with reference to particle size and carbon content. All as-made samples have a particle size in the range of 5–20 nm with a fcc structure, and show a soft ferromagnetic behavior. The samples become magnetically hard after annealing when they are converted to the fct structure. The law of approach to saturation was used to calculate the saturation magnetization and the magnetocrystalline anisotropy of samples with various vol % of C as a function of annealing time,[9] Figure 6 depicts these results, showing a universal trend of decreasing M_s with increased annealing time for each of the carbon contents considered. Though not definitive, there are two possible suspects that bring this about. These are related to either slight oxidation during sample processing or the lower magnetization of the ordered phase as also shown by the Mossbauer data (lower H_{hyp}).

Figure 7 shows that the anisotropy of the samples increases with annealing asymptotically approaching the value

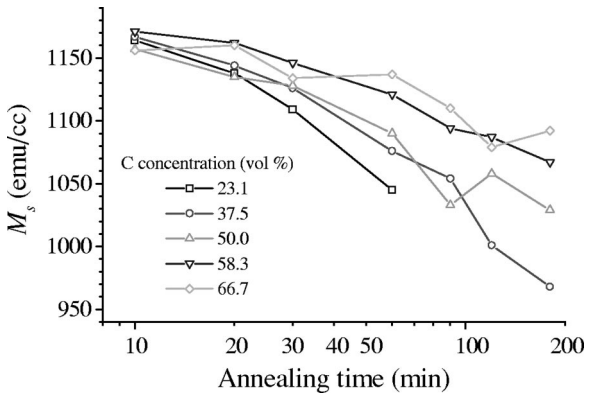

FIG. 6. M_s as a function of annealing time for several carbon contents.

of 10^7 ergs/cc, for annealing times up to 200 min. This value is significantly lower than the bulk value of the fully ordered FePt fct phase, consistent with the lower degree of atomic ordering found from the XRD results. The effect of the particle size on the Curie temperature (T_c) is shown in Fig. 8 for samples annealed at 600 °C for 30 min. A small decrease in T_c has been observed with decreasing size. The data follow a power law in close agreement with the prediction of the variation of T_c with particle size.[29]

Figure 9 shows hysteresis loops of FePt/C as a function of the vol % C in samples annealed at 600 °C for 20 min. As can be seen from the figure the loop squareness deteriorates with increasing C content. This behavior is expected when the distance between particles increases and the system approaches the idealized Stoner-Wohlfarth condition for noninteracting particles. Thus the increased squareness in samples with less carbon is attributed to exchange interactions between particles due to their proximity. For higher C content samples a decrease in coercivity is observed which is attributed to particles that are much below the single domain particle size approaching the superparamagnetic limit.

The coercivities measured are much lower than those predicted by Stoner-Wohlfarth,[30] where $H_c = 0.5(2K/M_s) = 100$ kOe for randomly distributed, non-interacting, single

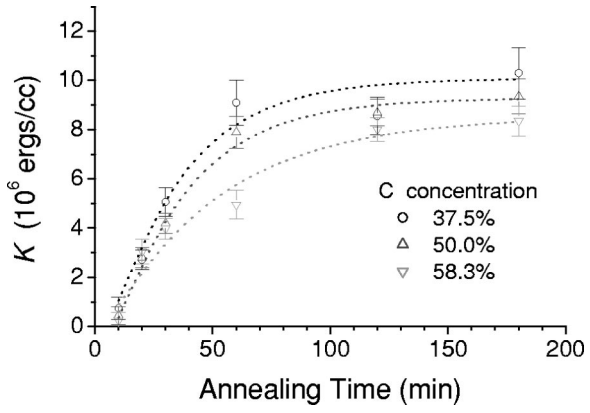

FIG. 7. Anisotropy as a function of annealing time for 37.5, 50.0, and 58.3 vol % C as determined from the law of approach to saturation.

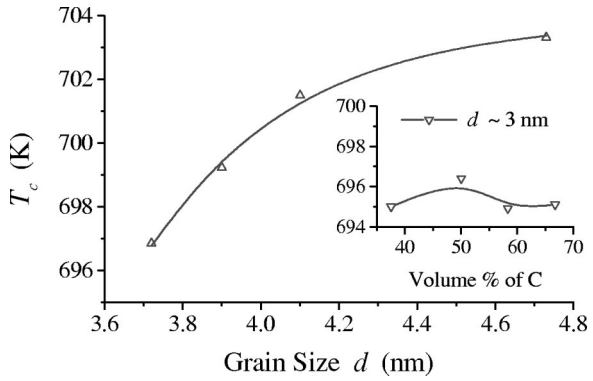

FIG. 8. T_c vs grain size for FePt/C annealed at 600 °C for 30 min. Inset shows the T_c variation with carbon content.

domain fct FePt. The lower values of coercivity are attributed mainly to the lower values of K related to incomplete atomic ordering and to a lesser extent to inter-particle exchange and thermal effects. Considering the effect of thermal fluctuations, the coercivity as a function of particle size D follows the relation

$$H_c(D) = 0.5H_k\left[1 - \left(\frac{D_p}{D}\right)^{3/2}\right],$$

where D_p is the superparamagnetic size and H_k the anisotropy field. Figure 10 shows a plot of H_c vs grain size for different values of C vol % and a fit to the theoretical curve

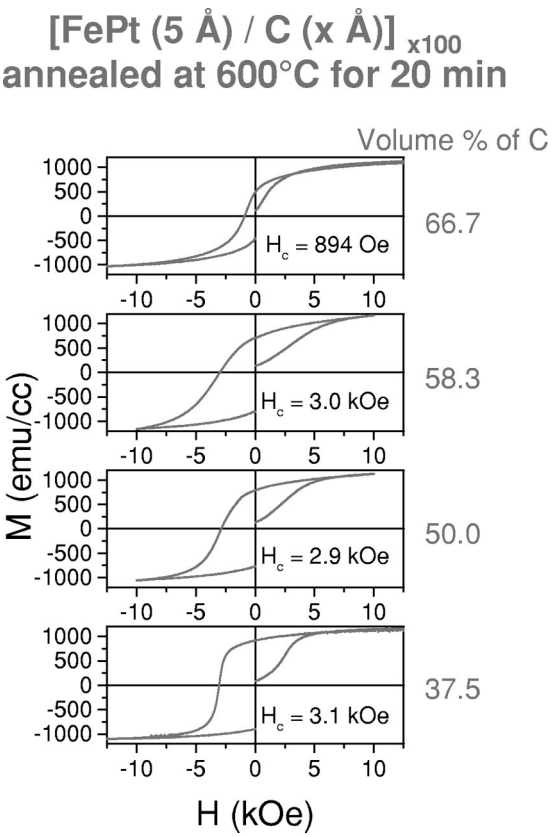

FIG. 9. Magnetization loops for a single annealing condition as a function of vol % C for samples annealed at 600 °C for 20 min.

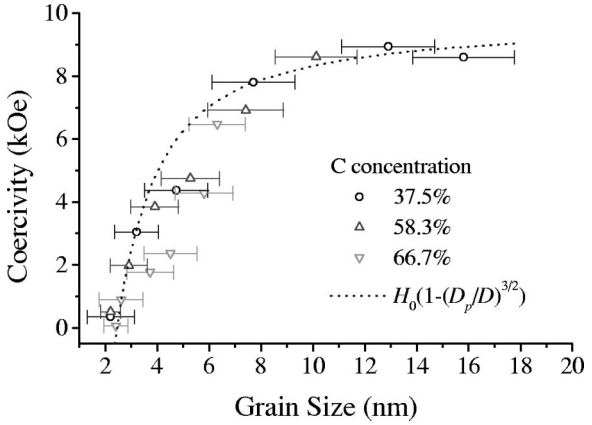

FIG. 10. Grain size as a function of coercivity for 37.5, 58.3 and 66.7 vol % C along with the theoretical curve for particle size dependence of coercivity.

shown as a dashed line. As can be seen there is a close fit of the data to the theoretical curve. The plot also gives an estimation of the superparamagnetic limit for the FePt system, which is about 2 nm.

As was discussed in the previous section, the degree of ordering increases with annealing time approaching but not quite reaching the fully ordered state within the experimental range of annealing parameters. To separate the degree of ordering and particle size contributions to coercivity, long duration annealing was performed on a sample with 80-vol % carbon where the particle size did not grow much (10–15 nm after 3 h at 800 °C). Figure 11 shows the hysteresis loop of this FePt/C sample. The coercivity is now significantly increased to a value of 34 kOe. Since the small particles are well separated, the increase in coercivity is mainly attributed to the increased degree of atomic ordering. It can be seen in the figure that there is a shoulder present in the hysteresis loop, indicative of the presence of a soft magnetic phase that is not exchange coupled to the hard phase. Despite the extended annealing time the material has not been fully transformed into the fct phase. This point is further elucidated in the discussion of the Mossbauer data.

Remanence curves provide insight into magnetic interactions through the use of the delta M formalism which classifies the nature of interactions present via the relation

$$\delta M = \overline{M_d}(H) - [1 - \overline{M_r}(H)],$$

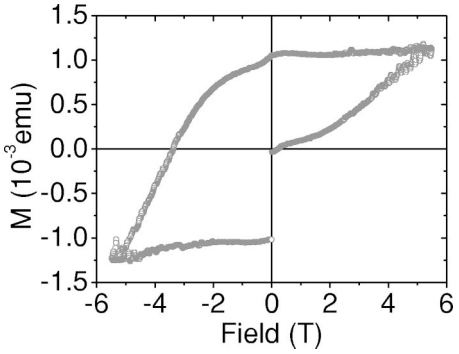

FIG. 11. FePt/C multilayer annealed for 3 h at 800 °C

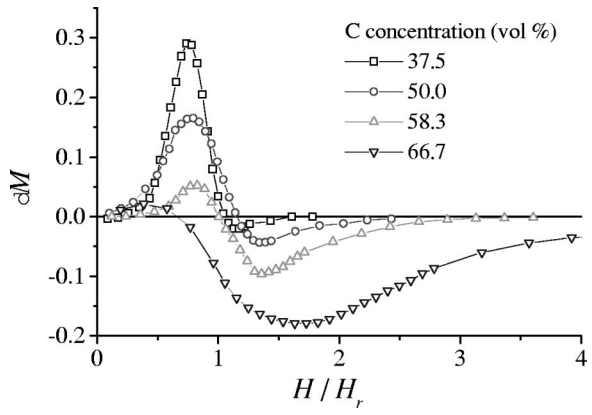

FIG. 12. δM plots for FePt/C samples with different carbon contents.

where M_r is the isothermal remanent magnetization and M_d is the dc demagnetization curve and the bar refers to reduced values normalized by $M_r(\infty)$. Figure 12 gives the δM curves for each of the vol % C levels considered in this study. As can be seen there is an obvious progression from exchange interactions ($\delta M > 0$) at low carbon content to magnetostatic interactions ($\delta M < 0$) as the amount of carbon in the samples is increased. As expected, the carbon serves to isolate the particles.

As the particle size is reduced, thermal fluctuations and the possibility of quantum tunneling of magnetization are expected to play a more dominant role in magnetization reversal. This phenomenon of magnetic viscosity can be used to determine the activation volume of a material. Quantum tunneling is ruled out for all carbon contents investigated, as there is no plateau[31] in the viscosity when plotted as a function of temperature. Hence we need only consider thermal fluctuations. Shown below in Fig. 13 is a plot of the activation volume as a function of vol % C determined from time dependent measurements taken with a reverse applied field close to the coercive field. There is a large disparity between the actual particle size and activation volumes for lower carbon content samples. As mentioned previously, these samples are exchange coupled as shown by the δM plots. It has been postulated that such a discrepancy in the activation

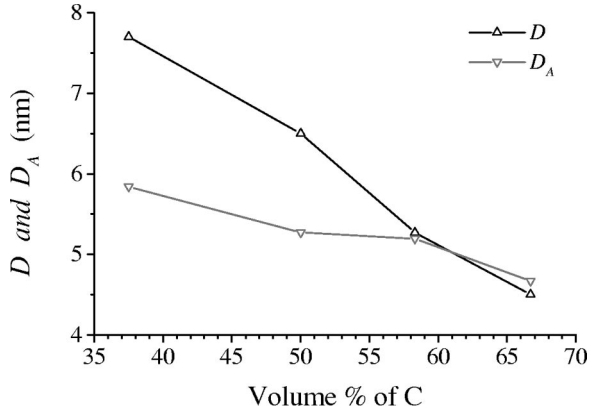

FIG. 13. Plot of the activation volume and actual particle size as determined by TEM.

TABLE II. Mossbauer parameters obtained from fits.

	Is shift	H_{hyp}	$E^2qQ/4$
Component I	0.29 mm/s	280 kOe	0.18 mm/s
Component II	0.29 mm/s	287 mm/s	0.07 mm/s

volume is indicative of incoherent magnetization reversal.[30] There is a convergence of the values of the activation volume and particle size with increasing carbon content. Consistent with structural investigations, the isolation of particles with increased carbon content suggests a coherent rotation reminiscent of an idealized Stoner-Wohlfarth system.[32]

Mossbauer spectroscopy was uaed to obtain further information at the atomic level. In all cases the spectra consist of a six-line pattern with asymmetries in intensities and linewidths, indicating more than one component. For some samples an additional quadrupole split paramagnetic component appears at RT, which turns to a magnetic component at LN temperature, as expected for small particles below the superparamagnetic limit. A set of samples with nominal bilayer thickness of 10-Å FePt/10-Å C displayed spectra fitted with two components with hyperfine parameters as shown in Table II. The parameters of the first component coincide with those of the tetragonal phase of FePt (fct $L1_0$) studied by Shinjo and Keune.[33] In particular the value of the quadrupole interaction is typical of this phase and corresponds to an aspect ratio of $c/a=0.96$. The parameters of the second component are more consistent the disordered cubic phase, as also indicated by the narrow distribution of the hyperfine field of ~ 10 kOe. However, there is still a small quadrupole interaction indicating a deviation from the cubic symmetry which may be the result of the onset of chemical ordering or the presence of interstitial carbon. Increasing the annealing time did not affect the hyperfine parameters but resulted in the growth of the first component at the cost of the second (the relative amount of the fct phase was 12%, 24%, 39%, and 44% for annealing periods of 2, 12, 30, and 90 min, respectively). This indicates that the fct phase is initially formed at the early stages of annealing and that continued annealing results in its growth. Thus the variation of the aspect ratio and the atomic ordering determined from the XRD data in reality just reflects a change due to the relative growth of the fct phase to produce an averaging over the larger sample.

Another set of samples with increased carbon content (nominal composition of the bilayer 10-Å FePt/25-Å C), displayed somewhat different behavior. The RT spectra were fitted with two magnetic and one paramagnetic component. The hyperfine parameters of the magnetic components were similar to the previously described set except that the fct phase is somewhat disordered, as indicated by a distribution of the hyperfine field of ~ 10 kOe, and the smaller quadrupole interaction (~ 0.14 mm/s) than the ideal value of 0.18 mm/s. The large quadrupole interaction (0.50 mm/s) seen in the paramagnetic component reflects the large surface to volume ratio expected for tiny particles observed in the C-rich samples. Annealing for periods between 2 and 90 min results in a decrease of the intensity of the paramagnetic component from 35% to 13% with a corresponding increase of the fct phase. Spectra taken at LN temperature for this set of samples do not display the paramagnetic component while the relative intensity of the fct phase has increased by the equivalent amount. A typical set of spectra comparing the RT and LN_2 measurements are shown in Figs. 14(a) and 14(b) respectively. These results indicate that in the carbon rich material small FePt particles are formed which display superparamagnetic behavior at RT for the Mossbauer time scale (10^{-8} sec). As shown by the LN measurement these particles are of fct-like nature; therefore, we can speculate that the formation of the fct phase originates in small particulate form. Furthermore, this observation clearly shows that tiny FePt particles (<4 nm) can undergo the fcc to fct transformation which was recently disputed by Ping *et al.*[34]

IV. CONCLUSIONS

Using the multilayer precursor technique described above we have been able to fabricate FePt nanoparticles in a C matrix and study their intrinsic and hysteretic properties as a function of particle size, which was varied as a function of carbon content and annealing conditions. The carbon content controls the kinetics of particle growth and mediates the magnetic interactions through the inter-particle distances.

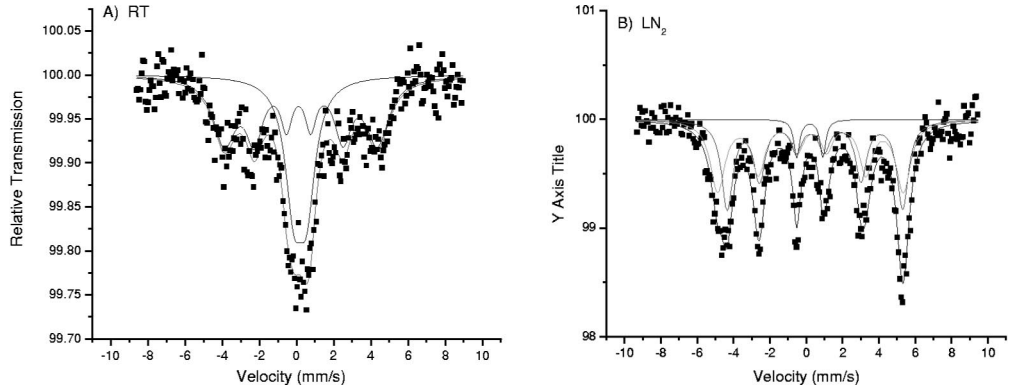

FIG. 14. Mossbauer spectra for FePt/C multilayer annealed at 700 °C for 2 min taken at (A) room temperature and (B) liquid nitrogen temperatures.

The above discourse hinges on the phase transformation from the disordered fcc to the ordered fct. From the data presented here this transformation occurs in very small particles (<4 nm) followed by the subsequent growth of the fct phase at the expense of the fcc material which progresses at a slow pace after the initial nucleation of fct. The coercivity can be tailored using the appropriate annealing conditions to vary the particle size and degree of atomic ordering. The lower values of coercivity are due to the presence of the lower anisotropy fcc phase even in the optimally prepared samples. This result poses immense promise for the magnetic recording industry in that high anisotropy materials can be produced well below current size requirements.

ACKNOWLEDGMENTS

The authors would like to thank C. Nelson at the Lawrence Berkeley National Laboratory for use of the Phillips 20CM FEG in acquiring some of the high resolution TEM images. This work was funded under NSF Grant No. DMR-9972035.

[1] L.F. Kneller and F.E. Luborsky, J. Appl. Phys. **34**, 656 (1963).
[2] D.L. Leslie-Pelecky and R.D. Rieke, Chem. Mater. **8**, 1770 (1996).
[3] D. Weller, A. Moser, L. Folks, M.E. Best, W. Lee, M.F. Toney, M. Schwickert, J-U. Thiele, and M.F. Doerner, IEEE Trans. Magn. **36**, 10 (2000).
[4] R. Krishnan and D.M. Porte, J. Magn. Magn. Mater. **168**, 15 (1997).
[5] K. Ouchi and N. Honda, IEEE Trans. Magn. **36**, 16 (2000).
[6] R.L. White, J. Magn. Magn. Mater. **209**, 1 (2000).
[7] E.E. Fullerton, D.T. Margulies, M.E. Schabes, M. Carey, B. Gurney, A. Moser, M. Best, G. Zeltzer, K. Rubin, and H. Rosen, J. Appl. Phys. **77**, 3806 (2000).
[8] J. Lohau, A. Moser, D.T. Margulies, E.E. Fullerton, and M.E. Schabes, Appl. Phys. Lett. **78**, 2748 (2001).
[9] S. Chikazumi, *Physics of Ferromagnetism*, 2nd ed. (Oxford University Press, New York, 1999).
[10] J.A. Christodoulides, P. Farber, M. Daniil, H. Okumura, G.C. Hadjipanayis, V. Skumryev, and D. Weller, IEEE Trans. Magn. **37**, 1292 (2001).
[11] S. Stavroyiannis, I. Panagiotopoulos, D. Niarchos, J.A. Christodoulides, Y. Zhang, and G.C. Hadjipanayis, J. Magn. Magn. Mater. **193**, 181 (1999).
[12] S. Stavroyiannis, I. Panagiotopoulos, D. Niarchos, J.A. Christodoulides, Y. Zhang, and G.C. Hadjipanayis, J. Appl. Phys. **85**, 4304 (1999).
[13] C.P. Luo, S.H. Liou, and D.J. Sellmyer, J. Appl. Phys. **87**, 6941 (2000).
[14] J.A. Christodoulides, Y. Zhang, G.C. Hadjipanayis, and C. Fountzoulas, IEEE Trans. Magn. **36**, 2333 (2000).
[15] M. Yu, Y. Liu, A. Moser, D. Weller, and D.J. Sellmyer, Appl. Phys. Lett. **75**, 3992 (1999).
[16] D.J. Sellmyer, C.P. Luo, M.L. Yan, and Y. Liu, IEEE Trans. Magn. **37**, 286 (2001).
[17] B. Bian, D.E. Laughlin, K. Sato, and Y. Hirotsu, IEEE Trans. Magn. **36**, 3021 (2000).
[18] S.C. Chen, P.C. Kuo, C.T. Lie, and T. Hua, J. Magn. Magn. Mater. **236**, 151 (2001).
[19] D.H. Ping, M. Ohnuma, K. Hono, M. Watanabe, T. Iwasa, and T. Masumoto, J. Appl. Phys. **90**, 4708 (2001).
[20] S. Ishio, N. Mori, T. Yoshino, H. Saito, T. Suzuki, and K. Mouchi, J. Magn. Magn. Mater. **235**, 148 (2001).
[21] S. Jeong, M.E. McHenry, and D.E. Laughlin, IEEE Trans. Magn. **37**, 1309 (2001).
[22] S.H. Liou, S. Huang, E. Klimek, R.D. Kirby, and Y.D. Yao, J. Appl. Phys. **85**, 4334 (1999).
[23] S. Stavroyiannis, I. Panagio Topoilos, D. Niarchos, J.A. Christodoulides, Y. Zhang, and G.C. Hadjipanayis, Appl. Phys. Lett. **73**, 3453 (1998).
[24] I. Panagiotopoulos, S. Satvroyiannis, D. Niarchos, J.A. Christodoulides, and G.C. Hadjipanayis, J. Appl. Phys. **87**, 4358 (2000).
[25] V. Karanasos, I. Panagiotopoulos, D. Niarchos, H. Okumura, and G.C. Hadjipanayis, Appl. Phys. Lett. **79**, 255 (2001).
[26] R.H. Kodama, J. Magn. Magn. Mater. **200**, 359 (1999).
[27] A. Cebollada, D. Weller, J. Sticht, G.R. Harp, R.F.C. Farrow, R.F. Marks, R. Savoy, and J.C. Scott, Phys. Rev. B **50**, 3419 (1994).
[28] B.E. Warren, *X-Ray Diffraction* (Dover, New York, 1990).
[29] R. Burgholz and U. Gradmann, J. Magn. Magn. Mater. **45**, 389 (1984).
[30] R.W. Chantrell, J. Magn. Magn. Mater. **95**, 365 (1991).
[31] X.X. Zhang, J. Tejada, J.M. Hernandez, and R.F. Ziolo, Nanostruct. Mater. **9**, 301 (1997).
[32] E.C Stoner and E.P. Wohlfarth, Proc. R. Soc. London, Ser. A **240**, 74 (1948).
[33] T. Shinjo and W. Keune, J. Magn. Magn. Mater. **200**, 598 (1999).
[34] D.H. Ping *et al.*, J. Appl. Phys. **90**, 4708 (2001).